Universities Council on Water Resources
Journal of Contemporary Water Research & Education
Issue 168, Pages 10-28, December 2019

Reduced and Earlier Snowmelt Runoff Impacts Traditional Irrigation Systems

*Yining Bai[1], Alexander Fernald[1], Vincent Tidwell[2], and Thushara Gunda[2]

[1]College of Agricultural, Consumer and Environmental Sciences, New Mexico State University, Las Cruces, NM
[2]Sandia National Laboratories, Albuquerque, NM
**Corresponding Author*

Abstract: Seasonal runoff from montane uplands is crucial for plant growth in agricultural communities of northern New Mexico. These communities typically employ traditional irrigation systems, called acequias, which rely mainly upon spring snowmelt runoff for irrigation. The trend of the past few decades is an increase in temperature, reduced snow pack, and earlier runoff from snowmelt across much of the western United States. In order to predict the potential impacts of changes in future climate a system dynamics model was constructed to simulate the surface water supplies in a montane upland watershed of a small irrigated community in northern New Mexico through the rest of the 21st century. End-term simulations of representative concentration pathways (RCP) 4.5 and 8.5 suggest that runoff during the months of April to August could be reduced by 22% and 56%, respectively. End-term simulations also displayed a shift in the beginning and peak of snowmelt runoff by up to one month earlier than current conditions. Results suggest that rising temperatures will drive reduced runoff in irrigation season and earlier snowmelt runoff in the dry season towards the end of the 21st century. Modeled results suggest that climate change leads to runoff scheme shift and increased frequency of drought; due to the uncontemporaneous of irrigation season and runoff scheme, water shortage will increase. Potential impacts of climate change scenarios and mitigation strategies should be further investigated to ensure the resilience of traditional agricultural communities in New Mexico and similar regions.

Keywords: *climate change, acequia, water resource management, system dynamics, irrigation valley*

Traditional agricultural communities have existed in New Mexico for hundreds of years (Hutchins 1928). These communities rely upon irrigation ditches called acequias, which divert available surface water from nearby streams, to maintain their pastoral lifestyle (Clark 1987). A majority of the water used for agricultural purposes in these communities has typically come from spring and early summer runoff produced by melting snowpack upstream of the irrigation community (Mote et al. 2005; LaMalfa and Ryle 2008; Rango et al. 2013). In recent years, data have shown that runoff produced by snowmelt has decreased, leading to less available water for the acequias in northern New Mexico (Rango et al. 2013; Harley and Maxwell 2018). The likelihood of future diminished snowpack in the southwest United States is supported by several studies (Thomas 1963; Mote et al. 2005; Rango et al. 2013; Mote et al. 2018).

Snowpack is the main source of surface water in New Mexico (Rango et al. 2013). Mountain snowpack accumulates during winter months and melts, producing runoff during spring and early summer. With increasing temperatures, the proportion of precipitation realized as snowfall is reduced, which impacts the timing and magnitude of the resulting runoff (Xiao et al. 2018).

Historically, drought impacts in NM were notable in 1900–1910, 1932–1937, 1945–1956, 1974–1977, 2002–2004, and 2011–2013 (Meyer 2018). Drought in New Mexico places stress on the agriculture. Drought is different from other natural hazards, since it occurs slowly and persistently (Thomas 1963). Meyer (2018) discussed that the current drought occurring in the Southwest is lurching into mega drought, which is prolonged for decades. Drought is caused by many factors (e.g., rising temperature, decreasing precipitation, diminished snowpack), which in turn increase the likelihood of severe wildfire. Drought adversely impacts the ecosystem and societal activities (such as agriculture) that are supported by the water system (Weiss et al. 2009). The duration and intensity of drought can be quantified with the Palmer Drought Severity Index (PDSI) (Weber and Nkemdirim 1998). PDSI is a popular meteorological drought index, which uses a water balance approach based on precipitation, temperature, and the local available water content (AWC) to quantify drought (Zargar et al. 2011). In ungauged areas where real-time runoff data are lacking, PDSI is able to improve drought monitoring and early warning due to its strong correlation with runoff (Tijdeman et al. 2018). Combining PDSI and stream flow simulation can be especially informative for agricultural practices during the irrigation season.

Hydrologic Modeling

Hydrologic models have been used to address variations in climate and soil properties and are useful for water resource management (Clarke 1973). Because limited infrastructure and available instrumentation exist in unpopulated mountainous areas, the modeling of watershed response to climate change is necessary to evaluate potential impacts on available water resources for downstream agriculture.

In order to make full use of hydrologic models, it may be useful to construct them in a fashion that allows future integration of the human dimension to the system. For this purpose, a hydrologic model alone is not sufficient. A system dynamics platform is helpful for integrating hydrologic models with future social dynamics (Gastelum et al. 2018; Tidwell et al. 2004, 2018). System Dynamics (SD) modeling is an integrated tool applied extensively in a broad range of natural resource management scenarios. SD involves the use of interconnected pathways representing changes of quantities over time (Gastelum et al. 2018). The underlying principle of SD is incorporation of feedback mechanisms. The method was developed as one way to conceptualize the physical world with interacting variables. It consists of stocks and flows to display a quantity footprint. Water can be influenced by factors such as population change, irrigation decision-making, and economic influences, which are typically not included in a hydrologic model (Scott 2018). The SD approach provides a solution to incorporate these factors into overall system simulations.

Research Objectives

The issues of climate change have been studied in many cases with large-scale watersheds. For example, the severity of flooding and drought both tend to increase over time, as indicated by climate change simulations in 12 major river basins in India with the Soil & Water Assessment Tool (SWAT) (Gosain et al. 2006), while a highly uncertain future was demonstrated by a model with 18 climate change scenarios in Iran (Farsani et al. 2018). Similarly, there is a need to understand the impact of climate change in small-scale watersheds, which are defined as smallest hydrologic units by the United States Geological Survey (USGS). Small irrigation communities, which rely on small-scale, upland watersheds are particularly vulnerable to the changes induced by climate changes due to limited water volumes and storage infrastructure in those regions. Shifting hydrological regimes caused by climate change can adversely affect the regional economy, human society, and ecosystem in traditional communities.

As described by Cruz et al. (2018), irrigation in traditionally managed communities in northern New Mexico is directly related to acequia flow, which originates from the upland watershed. The available irrigation and irrigation duration affect a community's decision regarding its farming and grazing schedule. Downstream community diverts water from runoff in the irrigation season; they also use forested uplands for grazing during the non-irrigation season. Precipitation and temperature shifts will affect upland pasture production and crop growth in irrigated land. Climate change could significantly impact the timing and length of the year available for farming and grazing practices.

This study examines potential impacts of climate change on runoff of an upland watershed and subsequent implications for irrigation management in the receiving downstream community. It is hypothesized that climate change will cause drier conditions after the mid-21st century. The SD model is expected to contribute a solid model base describing hydrologic processes to alternative management practices involving essential social and economic elements by simulating flow rate and schedule of runoff.

Materials and Methods

Study Area

The upland watershed feeding the El Rito, NM irrigation community is located in the Carson National Forest in northern New Mexico. This watershed forms a tributary to the Rio Chama, which flows to the Rio Grande. The area of the watershed is 188 km^2. The elevation ranges from 2113 to 3180 meters above sea level (Figure 1). The headwater sub-watershed is defined as the region that drains to USGS gauge 08288000 at El Rito, NM.

The irrigation community and irrigated lands of El Rito, NM are shown in Figure 2. It has been shown that there is a relationship between river runoff from upland watersheds and the water supply diverted into an acequia. The Census of Agriculture 2017 reports that the top crop in Rio Arriba County, where El Rito is located, is forage, and the top value in agricultural sales is cows and calves; irrigated pasture lasts from the end of April to October, when irrigation is indispensable (USDA 2019). Forage is not only an important source of sale income for local farmers, but also important for food storage for their livestock in the non-irrigation season (López et al. 2018).

El Rito receives more than 40% of its annual precipitation from July to October (Western Regional Climate Center 2009). Annual runoff sources vary throughout the year. Runoff from February to May is primarily from snowmelt, and runoff from June to September is primarily from monsoon rains. The average minimum and maximum historical monthly temperatures are 1.4 °C and 17.3 °C, respectively (Western Regional Climate Center 2009); the highest maximum temperatures are generally observed in August (34.33 °C) while the lowest minimum temperatures are observed in December (-16.95 °C).

Land cover is an important factor affecting interception, transpiration, and infiltration. Land use data were obtained from the Web Soil Survey (USDA NRCS 2017). The watershed was categorized into four classes: forest (mix/deciduous) (74.83%), evergreen forest (8.14%),

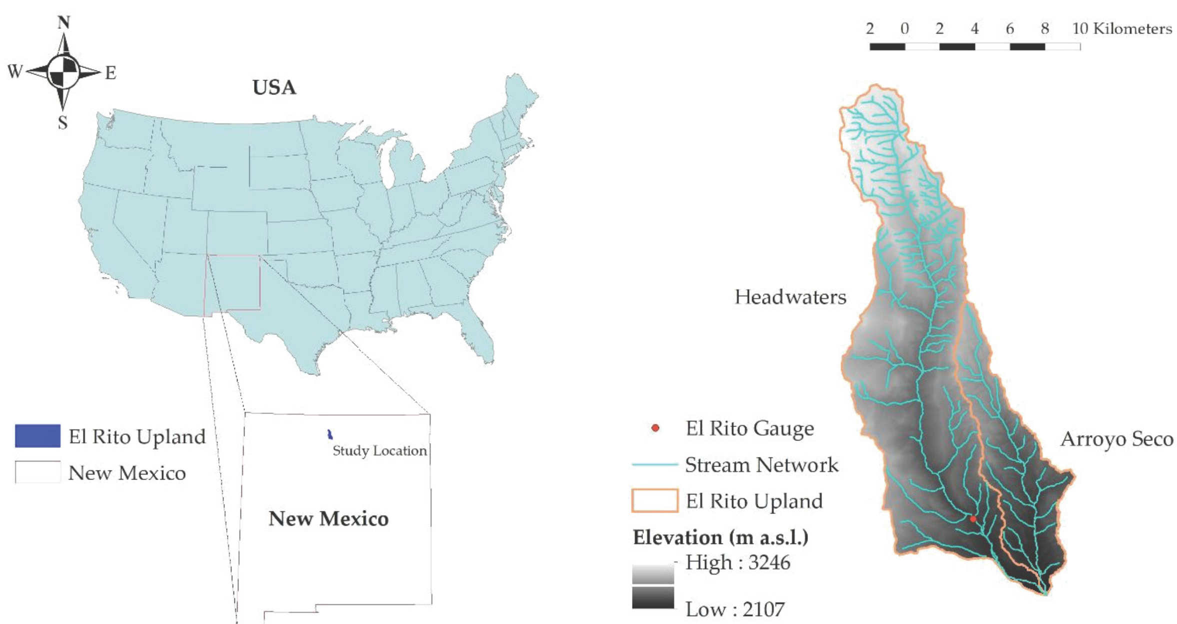

Figure 1. Upland watershed in El Rito consists of two sub-watersheds: the headwaters and the Arroyo Seco.

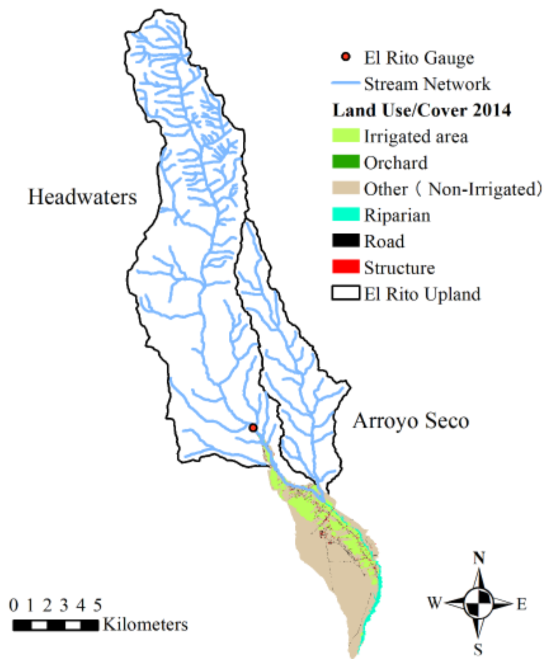

Figure 2. The land use of the irrigation community located downstream of the gauge: the upland watershed river feeds the downstream community (Sabie et al. 2018).

shrub land (6.18%), and grasslands/herbaceous (10.84%) (Figure 3). The soil types are clay (61.3%), loam (27.6%), and unweathered bedrock (11.1%). The entire watershed consists of two sub-watersheds, with the headwater watershed being defined by the USGS gauge placement. Runoff measurements at the gauge were made from 1930 to 1950 (U.S. Geological Survey 2019) and from 2010 to 2015 (Cruz et al. 2018). The measurements for river discharge (2010 to 2015) were collected directly adjacent to USGS gauge 08288000, above El Rito, NM.

Cruz et al. (2018) studied the relationship between upland river runoff and community ditches in northern New Mexico and concluded that every unit increase in river flow (cubic meter per second, m^3/s) leads to an increase in ditch flow. The relationship found between river-ditch flow by Cruz et al. (2018) ranged from 0.0561 to 0.1397. The ratio of 0.1397 was used to convert the simulated runoff from uplands into available irrigation supply (equation 2). The highest relationship ratio (0.1397) found by Cruz et al. (2018) was used to acquire a conservative estimate of the possibility of an irrigation water deficit in future scenarios.

Irrigation demand (equation 1) was calculated with community consumptive irrigation requirements (CIR) (cm/month) (Table 1) and the current agricultural land in the community (10.2 km^2). The monthly average irrigation demand during the irrigation season (April to October) was 1.2 m^3/s, used to compare with irrigation supply.

$$\text{Irrigation demand} = \text{Irrigated area} * \sum CIR \qquad (1)$$

Coefficient "α", was defined as a supply coefficient, which consists of irrigation supply and irrigation demand during the irrigation season to assess the supply level.

$$\alpha(t) = \frac{\sum_{\text{April}}^{\text{October}} \text{irrigation supply}}{\text{irrigation demand}} \qquad (2)$$

Data Collection

Climate and Hydrological Data. River discharge data were obtained for the years 2010 to 2015 (Cruz et al. 2018). Monthly climate datasets compiled for the SD model included precipitation and temperature data obtained from an area weather station and maintained by National Centers for Environmental Information (NCEI) (located at 36.3466°N, -106.1877°W), as well as climate projections from RCP scenarios 4.5 and 8.5 from HadGEM2-ES of the Coupled Model Intercomparison Phase 5 (CMIP5) model (Taylor et al. 2011). CMIP5 uses a weighted average method with a statistical downscaling approach applied to the General Circulation Model (GCM) (Taylor et al. 2011). RCP 4.5 and RCP 8.5 were chosen as they represent different concentration assumptions: the global emission peak is around 2040 in RCP 4.5, and the global emission continues to rise until the end of the 21st century in RCP 8.5. These two RCP's were selected to bracket future climate impacts. RCP 8.5 follows a business as usual case whereas RCP 4.5 addresses the case of concerted worldwide effort to reduce emissions. The whole simulation period was classified into three periods to capture the historical (1950–2000), current-term (2001–2049), and end-term (2050–2099).

Watershed Characteristics. A 30 m digital elevation model (DEM) was obtained from the USGS (U.S. Geological Survey 2016). Soils data

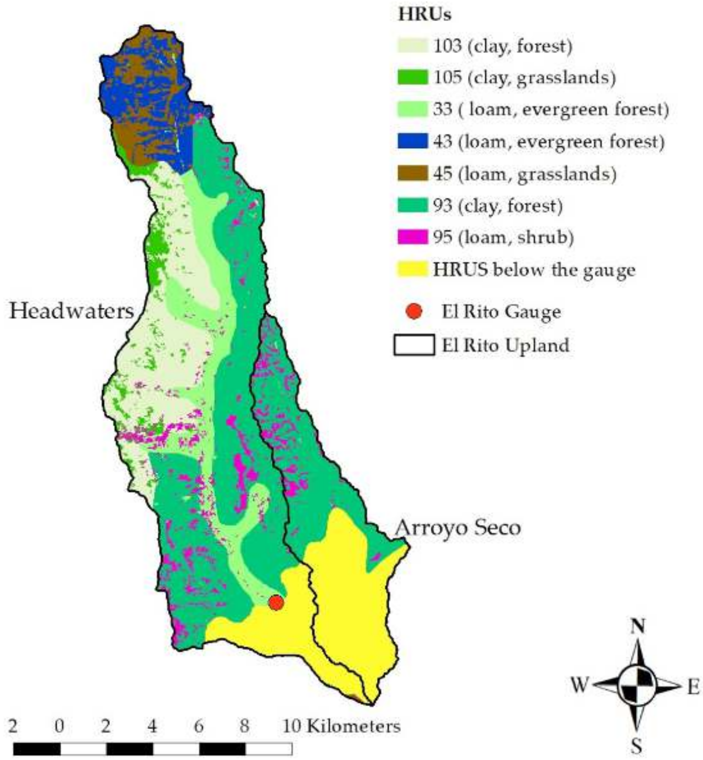

Figure 3. Hydrological response units in the El Rito study area. The eight HRUs represent the different soil texture and land cover combinations present in the region.

Table 1. Agricultural consumptive irrigation requirement (CIR) (cm/month) used in irrigation demand. Only months April through October are shown as the irrigation season.

April	May	June	July	August	September	October	Total
5.6	5.6	5.6	5.6	5.6	5.6	5.6	39.2

were provided by the Web Soil Survey (USDA NRCS 2017) (Table 2). The land use and land cover data were used to delineate hydrological response units (HRUs) (Table 3). The eight HRUs delineated distinct soil properties and vegetation combinations present in the El Rito watershed (Figure 3). The unique characteristics of soil and vegetation of each HRU determine interception, evapotranspiration, and infiltration rates in the hydrologic model components.

Hydrological Modeling

Description of SD Model. The simplified hydrology model was built on the platform of SD with the purpose of simulating hydrological flows (e.g., base flow and saturated excess flow) with the potential for adding future components such as human interactions (Winz et al. 2009). The hydrologic component of the SD model includes canopy capture, soil recharge, moisture storage, evapotranspiration, base flow, excess saturation runoff, and deep recharge. The hydrologic component is a continuous time model with a monthly time step. The model was physical-based (using climate and soil information) and suited to spatially and temporally large applications. The conceptualized diagram of the model based on interacting physical relationships is displayed in Figure 4.

The construction of the model was motivated by parsimony to capture the main hydrological processes. All governing equations are provided to explain the mass movement in the hydrologic cycle; this model was previously used to evaluate runoff in a similar watershed near Taos, NM (Gunda et al. 2018). Climate data from projections were provided in one eighth degree resolution and averaged by HRU for incorporation in the model. The SD model runs from 1950 to 2099, with the period from 2010 to 2015 (when runoff data were available) used for model calibration and validation. Calibration was conducted manually using the Powersim (Powersim Software AS, Bergen, Norway) (Powersim 2017) optimization tool to identify optimal soil coefficient parameters for each of the HRUs (Table 2).

Climate Change Projections

Projected Temperature. Climate projections indicate an increase in T_{mean} by about 2.67 °C and 3.77 °C in RCP 4.5 and RCP 8.5, respectively. Temperature increases are indicated across all

Table 2. Soil coefficient parameters used in calibrated model.

HRU	Porosity	Residual Water Content	Field Capacity	Wilting point	Conductivity
3	0.3	0.03	0.25	0.11	9
33	0.45	0.03	0.29	0.14	1.3
43	0.45	0.03	0.29	0.11	1.3
45	0.45	0.03	0.28	0.1	1.3
93	0.3	0.03	0.26	0.12	0.6
95	0.3	0.03	0.26	0.11	0.6
103	0.4	0.03	0.26	0.1	0.6
105	0.4	0.03	0.25	0.1	0.6

Note: HRU = hydrologic response unit.

Table 3. Eight hydrologic response units (HRU) representing soil and land cover information.

HRU	Area (%)	Soil Texture	Land Cover
3	9.2	Unweathered bedrock	Forest
33	15.8	Loam	Forest
43	8.1	Loam	Evergreen forest
45	6.4	Loam	Grassland
93	36.5	Sandy clay	Forest
95	6.1	Clay	Shrubland
103	19.7	Silt clay	Forest
105	3.5	Silt clay	Grassland

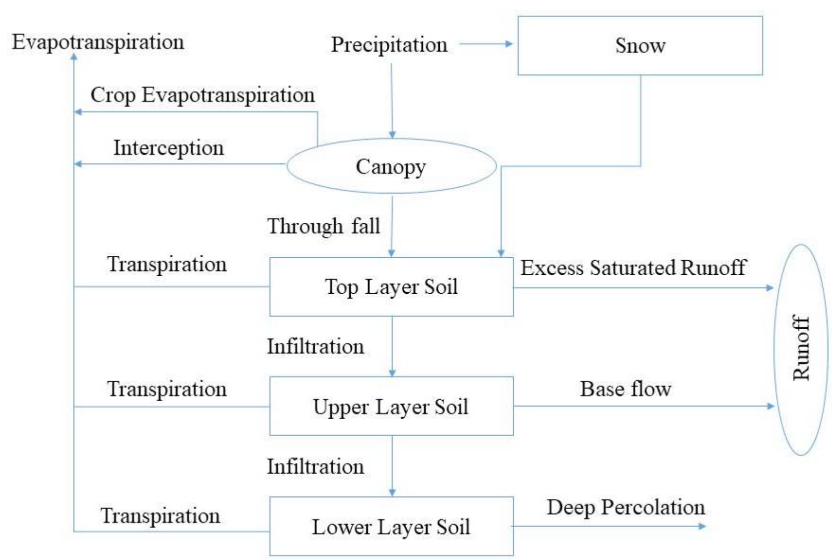

Figure 4. Primary dynamics included in the System Dynamics (SD) model. The SD model includes precipitation as rain or snow, interception, evapotranspiration, infiltration, deep percolation, excess saturation runoff, and base flow. Runoff generation includes both excess saturated runoff and base flow.

months in both scenarios (Figure 5), and monthly differences between maximum and minimum temperature enlarge from 17.6 °C historically (T_{max} 13.5 °C, T_{min} -4.1 °C) to 18.3 °C (T_{max} 17.4 °C, T_{min} -0.9 °C) and 18.5 °C (T_{max} 19.4 °C, T_{min} 0.9 °C) at the end of the simulation period under RCP 4.5 and RCP 8.5, respectively. The end-term projections of both scenarios show increased temperatures. Increased temperatures, particularly during winter and spring months, have implications on the amount and timing of snowfall and snowmelt runoff.

Projected Precipitation. Intra-annually, the El Rito upland watershed is characterized by three periods: dry season (October to February), snowmelt season (March to May), and monsoon season (June to September). RCP projections indicate a decrease in precipitation during the snow melting season for both terms relative to current conditions, which are more similar to historical conditions (Figure 6). During the monsoon and dry seasons, however, climate projections indicate increased precipitation for all terms of both scenarios compared with current and historical conditions. The seasonal precipitation shows the varied trends in three seasons. In both scenarios, the seasonal precipitation of the end-term has the largest standard error, which indicates the variability of precipitation in the future.

In RCP 4.5, the seasonal precipitation pattern throughout the year remains similar with historical records but has an increased magnitude. In the dry

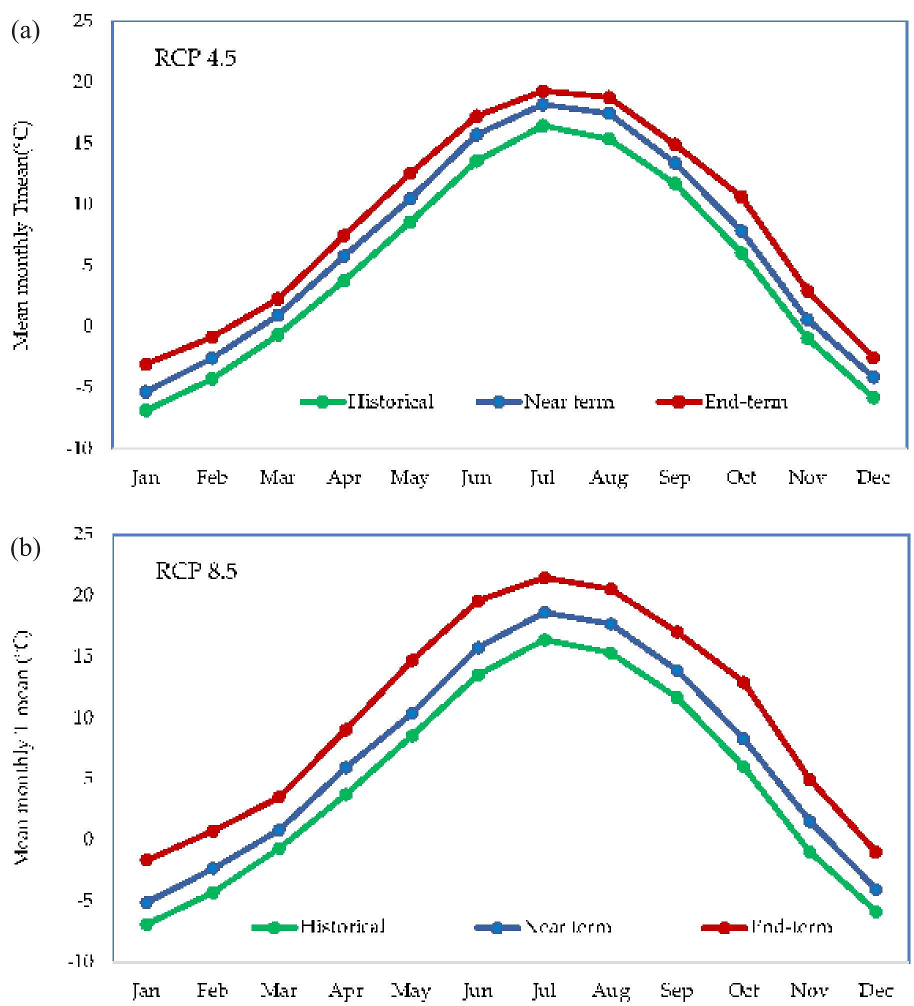

Figure 5. Projected mean temperature for the future in (a) representative concentration pathways (RCP) 4.5 and (b) RCP 8.5. Relative to the historical period, temperatures are consistently higher across the months in the future. Values represent historical (1950-2000) and projected, current term (2001-2049) and end-term (2050-2099) conditions.

season, precipitation is projected to increase by over 35% in the current-term and by over 20% in the end-term compared with historical conditions.

A notable difference of RCP 8.5 projections compared with RCP 4.5 is a smaller increase of precipitation during the dry and monsoon seasons of the current-term. Precipitation during the snow melting seasons is greater than historical conditions by over 30% in the current- and end-terms. Snow melting season precipitation in the end-term is predicted to be reduced from current conditions and be closer to historical conditions.

PDSI. PDSI was used to assess the severity and duration of drought. The Self-calibrating Palmer Drought Severity Index (sc-PDSI) DOS command line can be downloaded from the website (National Climatic Data Center 2003) and populated with parameters representing local conditions (AWC = 254 mm, station latitude = 36.5°N). The value of the PDSI is calculated to reflect how soil moisture compares to normal conditions.

Based on the drought classification, moderate drought and extreme drought will occur once the PDSI is lower than -2 and -4, respectively (United States Drought Monitor 2019). Long-term drought is defined as a duration of drought over six months and short-term drought has a duration of drought under six months (Northeast Regional Climate Center 2016). The drought percentage is calculated using the counts of drought occurrence and 12 months in a year. There is an increasing frequency of both short- and long-term, moderate and extreme drought in the future (Figure 7). Short-term moderate/extreme droughts could be

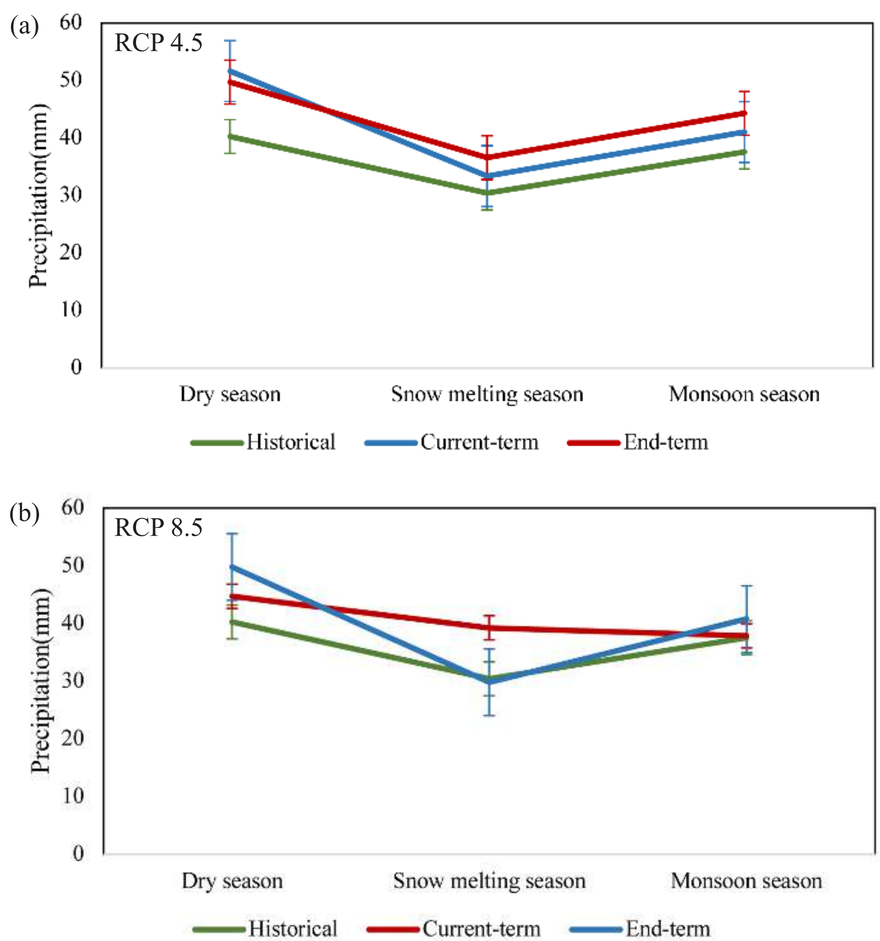

Figure 6. Seasonal precipitation trends in (a) representative concentration pathways (RCP) 4.5 and (b) RCP 8.5. Values represent historical (1950-2000) and projected, current term (2001-2049) and end-term (2050-2099) conditions.

a considerable risk in the current- and end-terms with a predicted frequency of over 40% in both scenarios. The total frequency over two duration categories and two drought categories are over 100, which means it will be likely to have not only short- or long-term drought with moderate or extreme levels simultaneously through one year but a combination of drought types and durations. In the end-term, under both scenarios, the extreme drought frequency reaches the highest frequency with RCP 4.5 and 8.5 reaching 47% and 63%, respectively. Overall, these scenarios show that drought will occur more often.

Results

Model Calibration and Validation

Model simulations of runoff indicate a pronounced spring peak (Figure 8), which ranges from 0.5 to 3.0 m^3/s, followed by summer peaks corresponding to large monsoonal precipitation events. Runoff generation that lags after rainfall events is less than two months. The coefficient of correlation between measured runoff and the simulated model runoff is 0.83 during the calibration period (2010–2011). The coefficient of correlation during the validation period (2012–2015) is 0.55.

Simulated Annual Runoff

In RCP 4.5, runoff increases are not as large as the projected precipitation increases (Table 4). With increases in precipitation, the runoff response ranges from 0.5% to 8.6% increase. In RCP 8.5, annual precipitation is again projected to increase for all terms, but simulated annual runoff shows increases in the current-term and a 24.7% decrease in the end-term. The changes in runoff are driven by higher temperatures, which drive increases in evapotranspiration (ET) rates over time.

Simulated Monthly Runoff

Simulation results indicate significant changes from the historical runoff regime at a monthly scale (Figure 9). Simulations from RCP 4.5 and

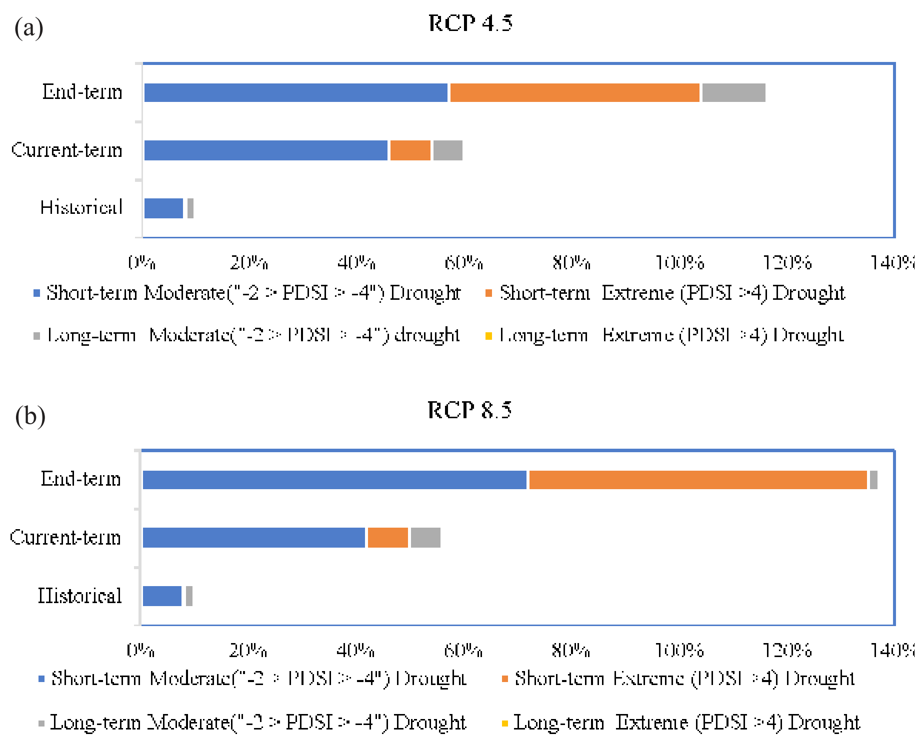

Figure 7. Short-term and long-term drought frequency (%) in (a) representative concentration pathways (RCP) 4.5 and (b) RCP 8.5. The y-axis represents the time from historical to the end-term. The drought frequency is analyzed in terms of duration and degree through one year. In the perspective of extreme and moderate drought, the frequency equals to 100%. Short-term drought could occur more than once through one year.

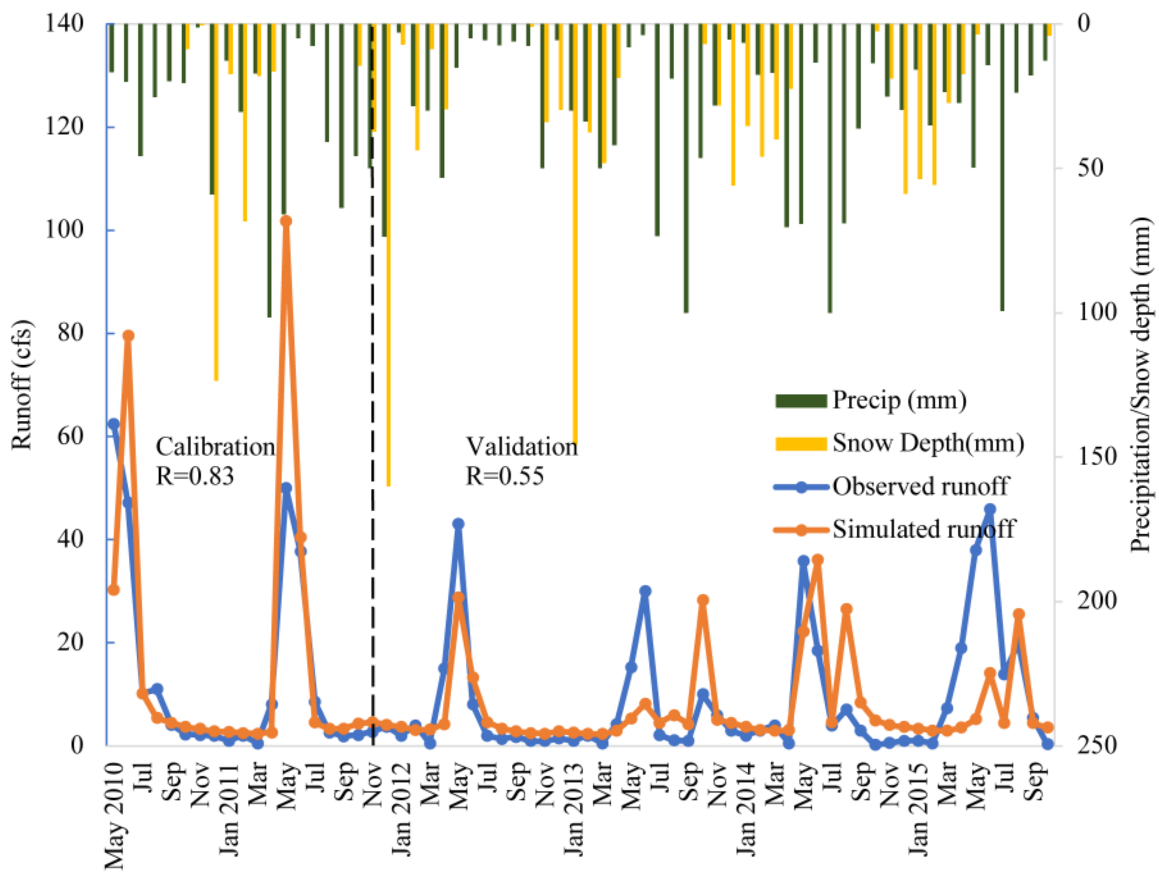

Figure 8. Model calibration and validation. The blue curve is observation and the orange curve is simulation with historical climate input. The green histogram represents the observed monthly precipitation depth and the yellow represents the simulated monthly cumulative snow water equivalent.

Table 4. Simulated runoff in the representative concentration pathways (RCP) 4.5 and RCP 8.5 scenario of HadGEM2-ES.

Value		----------- RCP 4.5 -----------		----------- RCP 8.5 -----------	
	Historical	**Current-term**	**End-term**	**Current-term**	**End-term**
Mean annual precipitation (mm)	439	523	535	493	501
ΔP (%)		18.8	21.8	12.1	14.0
Mean annual runoff (m^3/s)	5.5	6.0	5.5	5.8	4.1
ΔR (%)		8.6	0.5	5.1	-24.7
Mean annual evapotranspiration (ET) (mm)	266	315	337	306	331
ΔET (%)		27.0	18.4	24.4	14.9

8.5 show some disagreement in terms of volume and timing of runoff in the current-term. In RCP 4.5 it appears that conditions could stay similar to historical conditions in the current-term and show an increase in runoff during the snowmelt season in the end-term. Simulations of RCP 8.5 suggest an increase in runoff during the early two months of the snowmelt season in the current-term and a decrease in the end-term. Standard error shows that the runoff during March to June with RCP 4.5 and RCP 8.5 in the current-term has large variation when compared with other months.

Toward the end of the 21st century, simulations of both RCPs show several similar trends (Figure 9). End-term simulations of both projections show reduced runoff between the months of April and August, when agricultural activities are occurring. Historically, the runoff ranges from 0.3 to1.5 m^3/s from April to August. RCP 4.5 produces a runoff ranging from 0.3 to 1.0 m^3/s in the end-term; RCP 8.5 produces a runoff ranging from 0.4 to 0.6 m^3/s. Similarly, modeled results show snowmelt-induced runoff peaks shifting to earlier times of the year by up to one month and their magnitudes declining in the end-term. The largest decrease in modeled peak flow of the study area can be seen in the end-term of RCP 8.5 when the magnitude in peak flow is reduced by 55%.

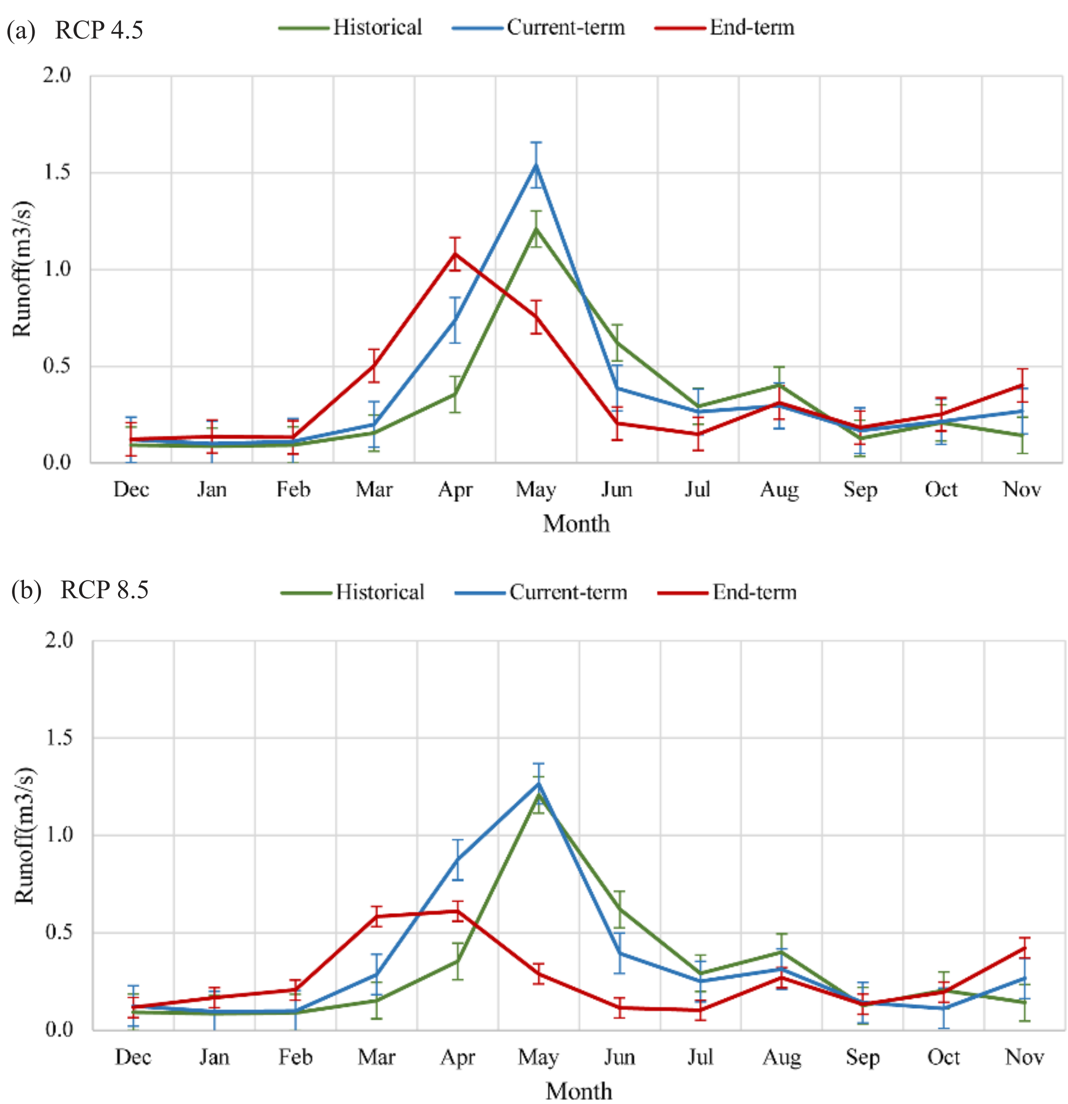

Figure 9. Monthly runoff: simulation projections and historical for (a) representative concentration pathways (RCP) 4.5 scenario and (b) RCP 8.5 scenario. The trends of runoff in the end-term of both scenarios are earlier and reduced.

Simulations of both projections show not only reductions in peak flow in the end-term, but decreases in total runoff from April to August (Figure 9). End-term simulations of RCP 4.5 suggest the total runoff from April to August decreases by 23%. End-term simulations of RCP 8.5 suggest that the runoff during these months decreases by 59%.

Another simulation result that is consistent between the two projections for all terms is increased runoff during the non-irrigation season, Marth to April (Figure 9). This is in part due to increased precipitation projections during these months. Warmer temperatures also lead to a higher percentage of precipitation during these months falling as rain and increased snowmelt. Though future dry season runoff is expected to be much greater than current conditions, the difference is small in relation to reductions in May to August runoff.

Water Balance Changes

The ratio of ET (including Evaporation (E) and Transpiration (T)), which increases by at least 14.9% in simulations, indicates an increase in the ratio of ET to precipitation in the current- to end-term simulations (Table 4). The increase in ET is expected due to projected increases in temperatures. Increases in winter and spring ET in the current- to end-term are in part responsible for predicted reductions in spring runoff. Another cause of reduced spring runoff appears to be an increase in the ratio of deep recharge to precipitation on an annual basis. Diminishing snowpack due to warmer temperatures is also evident (Table 5) as the ratio of snowpack reduces from 1.1% to 0.1%. The ratio of the snowpack is below 0.1% in the end-term of RCP 8.5. Both scenarios indicate a higher percentage of saturation excess runoff in some of the periods. The ratio of saturation excess runoff in all terms increases from historically 9.2% to at least 10.6% (Table 5), indicating more frequent short-interval, high-intensity rainfall events. Soil moisture levels are as low as 0.4% in all future periods compared to 4.9% historically (Table 5).

Irrigation Impacts

The number of frost-free dates in a given year is an indicator of the irrigation season length (Easterling 2002). Historically, El Rito had an average of 4.3 frost-free months per year (Table 6). The number of frost-free days increases with temperature in the RCPs over time. In the end-term of both scenarios, the frost-free duration is over one month longer than historically.

The graph of the water supply coefficient displays the trend of reoccurring stress on water availability through all periods (Figure 10). The current agricultural practices require a constant water supply through the irrigation season due to high ET crops (e.g., pasture and orchard) being grown in this arid area and region. In the end-term, water stress will continue to increase due to high ET rates and uncertainty in precipitation. A low water supply coefficient (<0.2) occurs frequently after 2040, in simulations.

Discussion

Trends in Future Hydrologic Regimes

A variety of hydrologic regime characteristics within the El Rito upland watershed could exhibit changes due to future climate conditions. Reduced runoff trends produced by the two considered climate scenarios were consistent with each other and concur with previous research of others (Rango et al. 2013; Buttle 2017; Coppola et al. 2018). Analysis of model drivers suggests that though precipitation and temperature are both expected to increase, the effect of the increase in precipitation could outweigh the negative effects of temperature on snowmelt runoff in the current-term.

An accordant trend between scenarios was that runoff will have altered timing, with the beginning and peak of spring runoff occurring much earlier in the year (Foulon et al. 2018; Hwang et al. 2018). Historically, peak runoff had been characterized by a single peak produced primarily from snowmelt in May. The difference between low flow in winter and high flow in spring was dependent upon winter and spring snowfall depth. Although climate projections showed a general trend of increasing annual precipitation, a shift in the timing of precipitation and a shift from snow to rain was predicted, which is in agreement with similar research (Fix et al. 2018).

A recent study by Chavarria and Gutzler (2018) in the Upper Rio Grande basin concluded that

Table 5. Water balance table of simulation (% of total precipitation).

		RCP 4.5		RCP 8.5	
	Historical	Current-term	End-term	Current-term	End-term
Snowpack	1.1	0.1	0.1	0.1	0.0
Rain evaporation	14.4	15.5	15.8	15.4	15.7
Snow evaporation	4.6	4.8	4.4	4.8	4.4
Soil evapotranspiration	58.7	60.1	60.4	60.0	61.1
Saturation excess runoff	9.2	11.2	11.2	11.5	10.6
Baseflow	6.1	6.0	5.8	6.0	5.9
Soil moisture	4.9	0.7	0.4	0.7	0.4
Deep recharge	1.1	1.5	1.9	1.5	1.9

Note: RCP = representative concentration pathway.

Table 6. Average frost-free months per year, when minimum temperature is above 0 °C.

	Historical	Current-term	End-term
RCP 4.5	4.3	4.8	5.8
RCP 8.5	4.3	4.8	6.2

Note: RCP = representative concentration pathway.

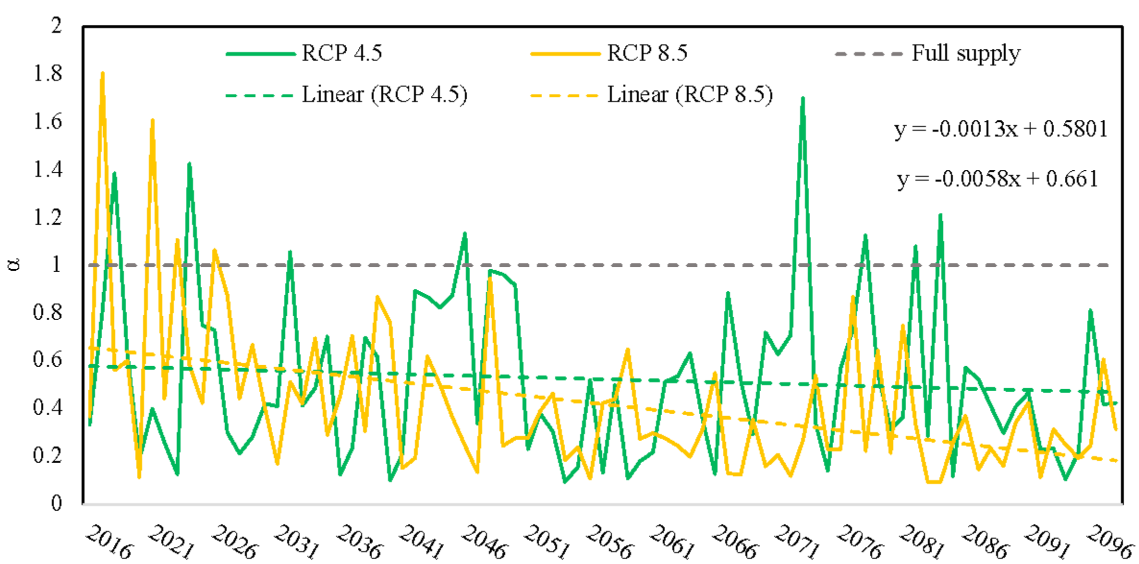

Figure 10. The water supply coefficient ranges from 0 to positive larger number. A coefficient closer to 0 means the water supply experiences significant stress; a coefficient over 1 means the water supply is sufficient. The slopes of two lines show that the water supply coefficient declines over time.

there has already been an observed reduction in April to July runoff attributable to increased winter and spring temperatures, decreased snow water equivalency, and a decreased relationship of runoff to precipitation since 1958. In the future, precipitation increases may moderate the runoff decline from diminished snowpack, but to date there is no evidence in actual observations (Udall and Overpeck 2017). Temperature strongly induces the runoff curtailment (Vano et al. 2014). The trend of snow pack diminution can be seen from climbing temperatures under both scenarios (Table 5). It would appear from simulations that a decreasing spring runoff trend is to be expected for the El Rito watershed in the end-term, and possibly sooner. End-term simulations of both climate scenarios showed reduced and earlier runoff in spring months, even though annual runoff was expected to increase for nearly all periods of both simulations.

Snowpack and soil moisture ratios decrease to less than 0.2% and 0.7% in both scenarios; the recharge ratio increases to 1.9% in the end-term of both scenarios (Table 5). Towards the end-term, the drought frequency in moderate and extreme level all exceed 40% (Figure 7). Even the precipitation in the end-term of RCP 8.5 is 14.0% more than historical, and the runoff decreases by 24.7% (Table 4). These analyses imply that the upland watershed is facing uncertainty in the timing and quantity of spring and early summer runoff due to unpredictable precipitation patterns and water distribution in hydrologic processes. Seasonal drought caused by climate change, such as diminished snowpack, higher temperatures, increased ET, and decreased soil moisture has been observed in other upland watersheds. Mao et al. (2015) used modeling and statistical approaches to analyze historical records of the snowpack, runoff, and other hydrological variables; they confirmed the correlation between warmer temperature and decreasing spring snowpack and runoff. It is widely recognized that ET will increase in scenarios that include a longer growing season and greater atmospheric demand in response to higher temperatures (Weiss et al. 2009; Serrat-Capdevila et al. 2011). Both scenarios produced increased ET (Table 4) and prolonged frost-free months (Table 6). Jung et al. (2010) discussed that a decrease in ET could be driven primarily by moisture limitation. The relation between soil moisture and ET corresponds with the trends in soil moisture and ET in Table 4 and Table 5. The increase in ET in the end-term of RCP 8.5 is 14.9%, which is less than the current-term (24.4%), but the precipitation in the end-term is slightly higher (Table 4). Soil moisture in the end-term of RCP 8.5 (0.4%) (Table 5) reflects the limitation of moisture on ET. Simulations in the context of this paper suggest that large increases in ET may cause uncertainty in runoff in the El Rito watershed, particularly toward the end-term. Though increased precipitation could offset effects of increased temperatures during some years, with increasing temperatures drought will be an inescapable reality. The phenomenon referred to as mega drought (Ault et al. 2016; Meyer 2018) is likely to occur in the current-term, even during years with average levels of precipitation, due to warmer temperatures, increased ET, and decreased soil moisture.

Management Implications

Model simulations support the conclusions of previous research (Rouhani and Leconte 2018) that there is potential for earlier and reduced runoff in spring and early summer. Results suggest a shift in the timing of spring runoff by over a month earlier than historically observed. Rather than focusing upon the timing of peak runoff, measures should be taken to cooperate with the trade-off between elements of practice, culture, and economy, and water availability to negate the effects of climate uncertainty (Hou et al. 2018).

New Mexico is experiencing water shortages for agricultural, ecological, and even domestic uses (Scarborough et al. 2018; Theimer et al. 2018). Shifts in runoff patterns that are suggested here could potentially lead to agricultural water shortages under current practices (Ahn et al. 2018). According to Cruz et. al. (2018), there are direct hydrologic connections between upstream rivers and downstream acequias in the irrigated communities of northern New Mexico. Residents who live in downstream areas might have to take adaptive actions to keep their agropastoral practices sustainable with limited water resources (López et al. 2018). Also, longer duration and increased drought from not only decreased precipitation, but also increases in temperature, or hot drought, could compound difficulties in agricultural practices. Investment in agricultural infrastructure, although not typical in the area, may be needed in the future to store and release water from intense precipitation events and runoff experienced during the winter.

The workforce for farming and grazing in the irrigation community is increasingly transitioning out of acequias to urban areas for better work and lifestyle opportunities (Benson et al. 2018). The enlarging gap between water demand and irrigation supply may intensify the trend of the workforce immigrating out of acequias, which reduces the sustainability of acequia communities in turn. In the end-term of both scenarios, water supply tends to be lower than 50% (Figure 10). The 50% water supply gap could indicate that the assumption of future water demand for farming and grazing may be substantially different from the past. With warmer climates, farmers might plant earlier in the season, which would change the timing of water demand. Similarly, recent modeling efforts have shown that the timing of water demand may not coincide with surface water deliveries (Cody 2018).

Prolonged periods of drought throughout a single year, and the increasing frequency of drought implies farmers may need to shift to crops which are tolerant to deficient irrigation practices and suitable for growing in winter months. Prolonged drought will likely have effects on the upland watershed in the long-term as well. This would have effects on the water supply to El Rito farmers. Prolonged drought could increase the rate of tree mortality and forest fires in forested areas (Daly et al. 2000; Hou et al. 2018). There could also be a long-term transition from larger species such as Ponderosa Pine (Pinus) to smaller trees such as Pinon Pine (Pinus) or Juniper (Juniperus) in areas that receive snowfall. This could potentially lead to small increases in summer and fall runoff from rain due to decreased interception. More importantly, reduced tree cover would lead to increased runoff after precipitation events and exacerbate the trend of reduced and shifted runoff (Wine and Cadol 2016).

Water supply coefficients, "α", is generally less than 1. "α", which in a few years is over one, indicates sufficient supply. The variation among years and seasons adds to the risk in water supply (Figure 10). In the future, the agricultural area will change as will the agriculture market. This requires adaptive agricultural practices such as modified crops and water-saving irrigation in order to cope with future potential drought while responding to social and market changes.

The unpredictable drought and prolonged frost-free periods will also change the water runoff supply to landscape and its timing, affecting the mechanism of farming and grazing in the watershed. Unpredictable drought not only affects the biomass production in publicly grazed forest, but also the hay production from farming for livestock. Thus, residential collaboration in traditional communities might become more necessary to maintain the sustainability of their grazing, farming, and rotational activities. Wehn et al. (2018) pointed out that engagement with the stakeholder in water management ensures social learning conditions, which foster the adaptive capabilities in decision-making. Richart et al. (2019) stated that with a multifunctional irrigation system, stakeholders could engage together to achieve good water governance by reducing tension, redirecting strategy, highlighting water scarcity, undertaking responsibilities, and sharing values among stakeholders. Konar et al. (2019) summarized the development of socio-hydrology; they pointed out that engagement with broader water management communities is a key opportunity for socio-hydrology to play a functional role in policy-making and scientific practice. Collaborative activities among stakeholders, communities, and institutes bring insight into science communication. They form the force crossing disciplines and scale to be more prepared to risk climate change brings.

Conclusion

Results suggest a general future trend of increasing annual runoff due to projected increases in annual precipitation. The most significant implications include shifts in runoff and precipitation regimes by the end of the 21st century. The two scenarios suggest hydrologic regimes that will deliver the majority of runoff from snowmelt up to one month earlier than historically observed. Simulations towards the end of the 21st century also suggest reduced snowmelt season runoff, during the time when irrigation activities are being performed. This could lead to operational water shortages later in the irrigation season.

Snowmelt dominated watersheds in northern New Mexico and southern Colorado have already shown earlier and reduced runoff during some recent years, suggesting climate change impacts are occurring. Though projections of precipitation show uncertainty as to annual and seasonal variability, projections of increased temperatures throughout the year appear likely. Regionally focused modeling, which couples hydrologic and social systems, could improve the resilience of local communities. Predictions of future potential risks caused by hydrologic regime changes could help communities develop management strategies before negative impacts are realized. Modeling efforts could also provide the ability to develop adaptive response strategies to avoid potential conflicts from competing demands for water. For those traditional agricultural communities without available advanced irrigation technologies and capital for large infrastructure, community-based and integrated management could be more flexible and practical for adapting to environmental changes, including future drought.

Acknowledgments

This research was funded by National Science Foundation Dynamics of Coupled Natural and Human Systems (CNH, No. BCS-1010516), the State of New Mexico Legislature (NMWRRI2018), and the New Mexico Agricultural Experiment Station. Costs to publish in open access were covered by New Mexico Water Resources Research Institute. The authors would like to thank Ian Hewitt for constructive comments. Sandia National Laboratories is a multi-mission laboratory managed and operated by National Technology and Engineering Solutions of Sandia, LLC, a wholly owned subsidiary of Honeywell International, Inc., for the U.S. Department of Energy's National Nuclear Security Administration under contract DE-NA0003525. The views expressed in the article do not necessarily represent the views of the U.S. Department of Energy or the United States Government.

Author Bio and Contact Information

Yining Bai (corresponding author) is a research assistant with New Mexico Water Resources Research Institute. Her research focuses on the impacts of climate change, socio-hydrology modeling, and water management. She can be reached at ynb@nmsu.edu.

Dr. Alexander Fernald is a Professor of Watershed Management. He currently serves as the director of the New Mexico Water Resources Research Institute. He is leading the institute in its mission to develop and disseminate knowledge that will assist the state, region, and nation in solving water resources problems. His primary research interests include water quality hydrology; land use effects on infiltration, runoff, sediment yield, and nonpoint source pollution; and effects of surface water/groundwater exchange on water availability and water quality. Dr. Fernald can be reached at afernald@nmsu.edu or Knox Hall 316, Las Cruces, NM 88001.

Dr. Vincent Tidwell is a Principle Member of the Technical Staff at Sandia National Laboratories. He has 22 years of experience conducting and managing research on basic and applied projects in water resource management, nuclear and hazardous waste storage/ remediation, and petroleum recovery. Most recently efforts have focused on establishing a multi-agency, multi-university center devoted to the creation and application of computer-aided decision support tools and stakeholder mediated decision processes. Focus of this effort is on water resource management and planning. Dr. Tidwell can be reached at vctidwe@sandia.gov.

Dr. Thushara Gunda completed her doctorate in Environmental Engineering at Vanderbilt and worked as a Postdoctoral Fellow at the Vanderbilt Institute for Energy & Environment. She also worked as an environmental consultant in Austin, TX, and earned B.S. and B.A. degrees in Environmental Science and Policy, respectively, at the University of Virginia. Her research interests involve systems-based, interdisciplinary research at the nexus of water, food, energy, and waste resources. She serves as senior member of Technical Staff at Sandia National Laboratories. She can be reached at tgunda@sandia.gov.

References

Ahn, S., S. Abudu, Z. Sheng, and A. Mirchi. 2018. Hydrologic impacts of drought-adaptive agricultural water management in a semi-arid river basin: Case of Rincon Valley, New Mexico. *Agricultural Water Management* 209: 206-218.

Ault, T.R., J.S. Mankin, B.I. Cook, and J.E. Smerdon. 2016. Relative impacts of mitigation, temperature, and precipitation on 21st-century megadrought risk in the American Southwest. *Science Advances* 2(10): e1600873.

Benson, M.H., R.R. Morrison, D. Llewellyn, and M. Stone. 2018. Governing the Rio Grande: Challenges and opportunities for New Mexico's water supply. In: *Practical Panarchy for Adaptive Water Governance: Linking Law to Social-Ecological Resilience*, B. Cosens and L. Gunderson (Eds.). Springer, pp. 99-114.

Buttle, J.M. 2017. Mediating stream baseflow response to climate change: The role of basin storage. *Hydrological Processes* 32(3): 363-378.

Chavarria, S.B. and D.S. Gutzler. 2018. Observed changes in climate and streamflow in the Upper Rio Grande Basin. *Journal of the American Water Resources Association* 54(3): 644-659.

Clark, I.G. 1987. *Water in New Mexico: A History of Its Management and Use*, University of New Mexico Press, Albuquerque, New Mexico.

Clarke, R.T. 1973. A review of some mathematical models used in hydrology, with observations on their calibration and use. *Journal of Hydrology* 19(1): 1-20.

Cody, K.C. 2018. Upstream with a shovel or downstream with a water right? Irrigation in a changing climate. *Environmental Science & Policy* 80: 62-73.

Coppola, E., F. Raffaele, and F. Giorgi. 2018. Impact of climate change on snow melt driven runoff timing over the Alpine region. *Climate Dynamics* 51(3): 1259-1273.

Cruz J.J., D.M. VanLeeuwen, A.G. Fernald, S.J. Guldan, and C.G. Ochoa. 2018. River-ditch hydrologic connections in a traditionally irrigated agricultural valley in New Mexico. *Journal of Irrigation and Drainage Engineering* 144(11): 04018032.

Daly, C., D. Bachelet, J.M. Lenihan, R.P. Neilson, W. Parton, and D. Ojima. 2000. Dynamic simulation of tree-grass interactions for global change studies. *Ecological Applications* 10(2): 449-469.

Easterling, D.R. 2002. Recent changes in frost days and the frost-free season in the United States. *Bulletin of the American Meteorological Society* 83(9): 1327-1332.

Farsani, I.F., M.R. Farzaneh, A.A. Besalatpour, M.H. Salehi, and M. Faramarzi. 2018. Assessment of the impact of climate change on spatiotemporal variability of blue and green water resources under CMIP3 and CMIP5 models in a highly mountainous watershed. *Theoretical and Applied Climatology* 136: 169-184.

Fix, M.J., D. Cooley, S.R. Sain, and C. Tebaldi. 2018. A comparison of U.S. precipitation extremes under RCP8.5 and RCP4.5 with an application of pattern scaling. *Climatic Change* 146(3): 335-347.

Foulon, É., A.N. Rousseau, and P. Gagnon. 2018. Development of a methodology to assess future trends in low flows at the watershed scale using solely climate data. *Journal of Hydrology* 557: 774-790.

Gastelum, J.R., G. Krishnamurthy, N. Ochoa, S. Sibbett, M. Armstrong, and P. Kalaria. 2018. The use of system dynamics model to enhance integrated resources planning implementation. *Water Resources Management* 32(7): 2247-2260.

Gosain, A.K., S. Rao, and D. Basuray. 2006. Climate change impact assessment on hydrology of Indian river basins. *Current Science* 90(3): 346-353.

Gunda, T., B.L. Turner, and V.C. Tidwell. 2018. The influential role of sociocultural feedbacks on community-managed irrigation system behaviors during times of water stress. *Water Resources Research* 54(4): 2697-2714.

Harley, G.L. and J.T. Maxwell. 2018. Current declines of Pecos River (New Mexico, USA) streamflow in a 700-year context. *The Holocene* 28(5): 767-777.

Hou, Y., M. Zhang, Z. Meng, S. Liu, P. Sun, and T. Yang. 2018. Assessing the impact of forest change and climate variability on dry season runoff by an improved single watershed approach: A comparative study in two large watersheds, China. *Forests* 9(1): 46.

Hutchins, W.A. 1928. The community acequia: Its origin and development. *The Southwestern Historical Quarterly* 31(3): 261-284.

Hwang, T., K.L. Martin, J.M. Vose, D. Wear, B. Miles, Y. Kim, and L.E. Band. 2018. Nonstationary hydrologic behavior in forested watersheds is mediated by climate-induced changes in growing season length and subsequent vegetation growth. *Water Resources Research* 54(8): 5359-5375.

Jung, M., M. Reichstein, P. Ciais, S.I. Seneviratne, J. Sheffield, M.L. Goulden, G. Bonan, A. Cescatti, J. Chen, R. de Jeu, A.J. Dolman, W. Eugster, D. Gerten, D. Gianelle, N. Gobron, J. Heinke, J. Kimball, B.E. Law, L. Montagnani, Q. Mu, B. Mueller, K. Oleson, D. Papale, A.D. Richardson, O. Roupsard, S. Running, E. Tomelleri, N. Viovy, U. Weber, C. Williams, E. Wood, S. Zaehle, and K. Zhang. 2010. Recent decline in the global land evapotranspiration trend due to limited moisture supply. *Nature* 467(7318): 951-954.

LaMalfa, E.M. and R. Ryle. 2008. Differential snowpack accumulation and water dynamics in aspen and conifer communities: Implications for water yield and ecosystem function. *Ecosystems* 11(4): 569-581.

López, S., A. Cibils, U. Smedly, S. Guldan, A. Fernald, C. Ochoa, K. Boykin, and L. Cibils. 2018. Linkages between acequia farming and rangeland grazing in traditional agropastoral communities of the Southwestern USA. *Sustainability* 10(6): 2021.

Mao, Y., B. Nijssen, and D.P. Lettenmaier. 2015. Is climate change implicated in the 2013-2014 California drought? A hydrologic perspective. *Geophysical Research Letters* 42(8): 2805-2813.

Meyer, R. 2018. The Southwest May Be Deep Into a Climate-Changed Mega-Drought. *The Atlantic*. Available at: https://www.theatlantic.com/science/archive/2018/12/us-southwest-already-mega-drought/578248/. Accessed April 13, 2019.

Mote, P.W., A.F. Hamlet, M.P. Clark, and D.P. Lettenmaier. 2005. Declining mountain snowpack in western North America*. *Bulletin of the American Meteorological Society* 86(1): 39-49.

Mote, P.W., S. Li, D.P. Lettenmaier, M. Xiao, and R. Engel. 2018. Dramatic declines in snowpack in the western US. *npj Climate and Atmospheric Science* 1(1): 2.

National Climatic Data Center. 2003. The GreenLeaf Project. Available at: http://greenleaf.unl.edu/. Accessed November 13, 2019.

Notheast Regional Climate Center. 2016. What is Long-Term Drought? Available at: http://www.nrcc.cornell.edu/services/blog/2016/12/06/index.html. Accessed November 13, 2019.

Powersim. 2017. Powersim Studio 10 Academic (64-bit), Powersim Software AS. Bergen, Norway.

Rango, A., C.M. Steele, E. Elias, J. Mejia, and A. Fernald. 2013. Potential impacts of climate warming on runoff from snowmelt: A case study of two mountainous basins in the Upper Rio Grande. AGU Fall Meeting, San Francisco, CA, December 9-13, 2013.

Rouhani, H. and R. Leconte. 2018. A methodological framework to assess PMP and PMF in snow-dominated watersheds under changing climate conditions – A case study of three watersheds in Québec (Canada). *Journal of Hydrology* 561: 796-809.

Sabie, R.P., A. Fernald, and M.R. Gay. 2018. Estimating land cover for three acequia-irrigated valleys in New Mexico using historical aerial imagery between 1935 and 2014. *The Southwestern Geographer* 21: 36-56.

Scarborough, V.L., S.G. Fladd, N.P. Dunning, S. Plog, L.A. Owen, C. Carr, K.B. Tankersley, J.-P. McCool, A.S. Watson, E.A. Haussner, B. Crowley, K.J. Bishop, D.L. Lentz, and R.G. Vivian. 2018. Water uncertainty, ritual predictability and agricultural canals at Chaco Canyon, New Mexico. *Antiquity* 92(364): 870-889.

Scott, R. 2018. A systems perspective on the natural resources framework: Comment on Hearnshaw et al. *Policy Quarterly* 10(4): 59-62.

Serrat-Capdevila, A., R.L. Scott, W.J. Shuttleworth, and J.B. Valdés. 2011. Estimating evapotranspiration under warmer climates: Insights from a semi-arid riparian system. *Journal of Hydrology* 399(1-2): 1-11.

Taylor, K.E., R.J. Stouffer, and G.A. Meehl. 2011. An overview of CMIP5 and the experiment design. *Bulletin of the American Meteorological Society* 93(4): 485-498.

Theimer, T.C., M.K. Sogge, S.N. Cardinal, S.L. Durst, and E.H. Paxton. 2018. Extreme drought alters frequency and reproductive success of floaters in Willow Flycatchers. *The Auk* 135(3): 647-656.

Thomas, H.E. 1963. *Effects of Drought in the Rio Grande Basin: Drought in the Southwest 1942-56*. Geological Survey Professional Paper 372-D. United States Department of the Interior. U.S. Government Printing Office, Washington, D.C.

Tidwell, V.C., B.D. Moreland, C.R. Shaneyfelt, and P. Kobos. 2018. Mapping water availability, cost and projected consumptive use in the eastern United States with comparisons to the west. *Environmental Research Letters* 13: 014023.

Tidwell, V.C., H.D. Passell, S.H. Conrad, and R.P. Thomas. 2004. System dynamics modeling for community-based water planning: Application to the Middle Rio Grande. *Aquatic Sciences* 66(4): 357-372.

Tijdeman, E., L.J. Barker, M.D. Svoboda, and K. Stahl. 2018. Natural and human influences on the link between meteorological and hydrological drought indices for a large set of catchments in the contiguous United States. *Water Resources Research* 54(9): 6005-6023.

Udall, B. and J. Overpeck. 2017. The twenty-first century Colorado River hot drought and implications for the future. *Water Resources Research* 53(3): 2404-2418.

U.S. Department of Agriculture (USDA). 2019. National Agricultural Statistic Service: Quick Stats. Available at: https://quickstats.nass.usda.gov/. Accessed March 2, 2019.

U.S. Department of Agriculture, Natural Resources Conservation Service (USDA NRCS). 2017. Web Soil Survey. Available at: https://websoilsurvey.sc.egov.usda.gov/App/HomePage.htm. Accessed October 30, 2019.

United States Drought Monitor. 2019. Drought Classification. Available at: https://droughtmonitor.unl.edu/About/AbouttheData/DroughtClassification.aspx. Accessed Octover 30, 2019.

U.S. Geological Survey. 2016. USGS NED 1/3 arc-second n49w092 1 x 1 degree ArcGrid 2016. Available at: https://viewer.nationalmap.gov/basic/. Accessed November 28, 2018.

U.S. Geological Survey. 2019. Surface Water Data for USA: USGS Surface-Water Monthly Statistics. Available at: https://waterdata.usgs.gov/nwis/monthly?. Accessed September 23, 2019.

Vano, J.A., B. Udall, D.R. Cayan, J.T. Overpeck, L.D. Brekke, T. Das, H.C. Hartmann, H.G. Hidalgo, M. Hoerling, G.J. McCabe, K. Morino, R.S. Webb, K. Werner, and D.P. Lettenmaier. 2014. Understanding uncertainties in future Colorado River streamflow. *Bulletin of the American Meteorological Society* 95(1): 59-78.

Weber, L. and L. Nkemdirim. 1998. Palmer's drought indices revisited. *Geografiska Annaler: Series A, Physical Geography* 80(2): 153-172.

Wehn, U., K. Collins, K. Anema, L. Basco-Carrera, and A. Lerebours. Stakeholder engagement in water governance as social learning: Lessons from practice. *Water International* 43(1): 34-59.

Weiss, J.L., C.L. Castro, and J.T. Overpeck. 2009. Distinguishing pronounced droughts in the southwestern United States: Seasonality and effects of warmer temperatures. *Journal of Climate* 22: 5918-5932.

Western Regional Climate Center. 2009. El Rito, New Mexico- Climate Summary. Available at: https://wrcc.dri.edu/cgi-bin/cliMAIN.pl?nmelri. Accessed February 21, 2019.

Wine, M.L. and D. Cadol. 2016. Hydrologic effects of large southwestern USA wildfires significantly increase regional water supply: Fact or fiction? *Environmental Research Letters* 11(8): 085006.

Winz, I., G. Brierley, and S. Trowsdale. 2009. The use of system dynamics simulation in water resources management. *Water Resources Management* 23(7): 1301-1323.

Xiao, M., B. Udall, and D.P. Lettenmaier. 2018. On the causes of declining Colorado River streamflows. *Water Resources Research* 54(9): 6739-6756.

Zargar, A., R. Sadiq, B. Naser, and F.I. Khan. 2011. A review of drought indices. *Environmental Reviews* 19(NA): 333-349.